International Journal of
Automotive Manufacturing and Materials（IJAMM）

Scilight

Article

Study on Naphtha Combustion in HCCI Engines

An Lu [1], Junior James Achumu [2], and Junfeng Yang [2,*]

[1] School of Mechanical Engineering, Shanghai Jiao Tong University, Shanghai 200240, China
[2] School of Mechanical Engineering, University of Leeds, Leeds LS2 9JT, UK
* Correspondence: j.yang@leeds.ac.uk
Received: 15 July 2024; Revised: 18 October 2024; Accepted: 22 October 2024; Published: 28 October 2024

Abstract: The chemical kinetics model studies have been conducted in this paper to assess ignition characteristics of coal-based naphtha (with carbon range C_3–C_{10}, RON of 54) for use in advanced engines. Reactivity of coal-based naphtha (CBN) was compared with two surrogate models: PRF54 (46 mole% n-heptane/54 mole% iso-octane) model and 3-component (42.561 mole% NC_7H_{16}, 43.683 mole% IC_8H_{18} and 13.756 mole% IC_6H_{14}) model. Both two models reasonably predicted the ignition delay times (IDTs) of CBN at 10, 15 bar and 640–900 K. In addition, the experimental and simulation study of coal-based naphtha HCCI combustion was carried out. CHEMKIN-PRO software was used to simulate the effects of intake temperature (T_{in}) and equivalent ratio (Φ) on the combustion process of naphtha HCCI engine. The results show that the combustion of coal-based naphtha HCCI is sensitive to the T_{in}. With the increase of T_{in}, the combustion phase of HCCI is obviously advanced, the concentration of OH and HO_2 increases in the middle and low temperature reaction process, and the corresponding curve moves forward as a whole. The change of Φ has little effect on the concentration of OH and HO_2 before ignition, and the change of ignition time with the mixture concentration is not obvious. It should be pointed out that when the T_{in} is high or mixture is rich, the coal-based naphtha HCCI engine is prone to knock, and the peak phase will appear before top dead center (TDC). This phenomenon is especially obvious when the T_{in} is very high. It can be seen that the coal-based naphtha is suitable for low-temperature lean combustion.

Keywords: coal-based naphtha; HCCI; chemical kinetics; Ignition delay time; engine modelling

1. Introduction

Under the dual pressure of energy and environment, it is urgent to explore new alternative energy for vehicles. Naphtha as an intermediate production in crude oil refining has attracted more and more attention. Because the ignition delay time of naphtha is longer than diesel, naphtha provides full mixing and proper chemical propensity. Naphtha as a low-octane fuel (with Research Octane Number (RON) in 50 – 70) is considered as an alternative fuel for advanced combustion modes [1–4].

Engine low-temperature combustion technology is a new combustion technology, which makes full use of fuel energy and reduces emissions. Han et al. [5–7] studied the load extension and emissions (HC, CO, NO_x and soot) of diesel and gasoline blended fuel under low-temperature combustion, and the test results showed the potential of low-temperature combustion in compress ignition of fuel. Homogeneous Charge Compression Ignition (HCCI) is considered as a promising combustion mode because of its low-temperature lean combustion characteristics.

The development and verification of chemical reaction mechanism need the fundamental combustion data of fuel. Considering the complex composition of fuels such as gasoline, diesel, and naphtha, researchers often formulate simple surrogate, including several key components, to simulate the ignition and combustion characteristics of real fuels. Alabbad et al. [8,9] and Javed et al. [1,10] measured the ignition delay time (IDT) of several naphtha over a wide range of temperatures, pressures, and equivalence ratios. According to the specific physical and chemical properties of the target naphtha, multi-component surrogates consisting of

n-alkanes (n-butane, n-pentane, n-heptane), iso-alkanes (iso-pentane, 2-methylhexane, iso-octane), cycloalkanes (cyclopentane, cyclohexane), aromatic hydrocarbons (toluene, 1, 2, 4-tritoluene) and alkenes (1-hexene) were proposed. Due to the similar composition of gasoline and naphtha, n-heptane/isooctane, as the Primary Reference Fuel (PRF), is the most common surrogate for gasoline, and PRF was tested and compared in studies. The results showed that PRF can predict the IDT of naphtha well at medium and high temperature, but the reactivity of PRF is higher than that of naphtha at low temperature. This is because compared with n-heptane and isooctane, naphtha contains a larger proportion of small molecule n-alkanes and iso-alkanes. Compared with PRF, the multi-component surrogate can better predict the reactivity of naphtha at low temperature. Li et al. [11] measured the IDT of naphtha with RON of 72 and 83 on rapid compression machine (RCM), and compared it with the study of Alabbad et al. [8]. The results showed that the fuel had similar RON but different IDT. Just matching RON is not enough when building the surrogate model. In addition, Wang [12] constructed two 3-component models with different mixing ratios of n-heptane, isooctane and methylcyclohexane to characterize light naphtha. One model matches the RON and Motor Octane Number (MON) of light naphtha, and the other model matches the RON and H/C ratio. The ignition characteristics of light naphtha and the two surrogates are studied at the pressure of 10–30 bar on the RCM. The results showed that IDT of light naphtha can be better predicted by the surrogate matching RON and H/C ratio. Ahmed et al. [13] developed a multi-component surrogate for light naphtha fuel using a multivariable nonlinear constrained optimization method, and studied the spontaneous combustion characteristics of light naphtha and its surrogate in a constant volume combustion chamber. Zhong et al. [14] carried out experimental and kinetic studies on the pyrolysis and oxidation of a light naphtha fuel and its substitute. Based on the chemical functional group method, a 3-component model of 64.2 mol% isopentane, 21.0 mol% n-hexane and 14.8 mol% methylcyclopentane was proposed to simulate the target naphtha.

The existing chemical kinetic models of naphtha are mainly built for petroleum-based naphtha. However, the hydrocarbon composition of coal-based naphtha differs greatly from that of petroleum-based naphtha. There are few studies on the chemical kinetics of coal-based naphtha. Lu et al. [15] studied the HCCI combustion characteristics and knock of coal-based naphtha, but did not study its fundamental combustion characteristics and chemical kinetics. Compared with petroleum-based naphtha, coal-based naphtha has very few cycloalkanes and almost no olefins and aromatic hydrocarbons. This determines its more potential in reducing engine emissions.

Fundamental combustion data is very important for developing and verifying the chemical reaction kinetics of coal-based naphtha. Therefore, it is necessary to study the fundamental combustion characteristics of coal-based naphtha and build its surrogate model to study the chemical reaction kinetics. In this study, PRF (n-heptane/isooctane) and 3-component surrogate were proposed to simulate the IDT of real coal-based naphtha. The 3-component surrogate model was built by matching RON and H/C ratio. The IDT of the two surrogate models were compared with the experimental data. In addition, in order to better understand the low-temperature ignition behavior of coal-based naphtha, the low-temperature chemical reactions of two surrogate models were analyzed. Finally, the combustion model of coal-based naphtha was employed to simulate a HCCI combustion engine. And the optical of HCCI fueled by naphtha has been performed.

2. Methodology

2.1. Fuel Properties and Detailed Hydrocarbon Analysis

The coal-based naphtha (CBN) studied in this paper is provided by China Energy Group Ningxia Coal Industry Co., LTD. Table 1 lists the important thermo-physical parameters such as lower heating value, density and viscosity. The fuel has a lower octane number (research octane number RON 54), and an average molecular formula of $C_{6.97142}H_{15.88244}$.

Table 1. Thermo-physical parameters of coal-based naphtha [15].

Properties	Coal-based naphtha
Average chemical formula	$C_{6.97142}H_{15.88244}$
Research octane number (RON)	54
Lower heating value (MJ/kg)	45.73
Density at 20 °C (g/cm^3)	0.67
Kinematic viscosity at 20 °C (mm^2/s)	0.56
Sulfur content (mg/kg)	<1
Nitrogen content (mg/kg)	<1
Water content (mg/kg)	356

Shell Technology Centre (Amsterdam) conducted Gas Chromatography for Detailed Hydrocarbon Analysis (GCDHA) on this coal-based naphtha to determine its specific composition. The results of GCDHA are provided in [16]. It can be seen that $C_3 - C_{10}$ hydrocarbons mainly consist of n-alkanes (20.182%), iso-alkanes (75.641%) and cycloalkanes (3.784%), without any oxygen-containing substances, olefins and aromatic hydrocarbons. From the results of GCDHA, it is obvious that coal-based naphtha has different properties and composition from petroleum naphtha containing a certain amount of olefins and aromatic hydrocarbons [8,14]. This also determines that it has great potential in reducing emissions. The existence of olefins and aromatic hydrocarbons is very serious to the environment pollution. The international standard controls the content of aromatics and alkenes in fuel strictly, because they are very easy to form the gel inside the car and carbon deposition phenomenon, thus affecting the normal work of the engine, reducing efficiency and increasing fuel consumption, and emission deterioration.

2.2. Surrogate Formulation

There are several methods to select the components of fuel surrogate: Mehl et al. [17], Ahmed et al. [18] and Pera et al. [19] have all proposed methods for the selection of fuel surrogate. At present, functional groups, molecular weight, H/C ratio, octane number, density, boiling point and distillation characteristics are mainly considered in the selection of fuel surrogate components. Pitz et al. [20] proposed the following principles for the selection of fuel surrogate components: First, the selected components should match or reflect the thermal properties of the characterized fuel without too much difference; secondly, the selected components should have a certain research basis in the early stage (that is, the chemical reaction mechanism related to the selected components has been fully studied and verified), so as to be used in the construction and verification of chemical kinetic models; the last is to satisfy the principle of practicality.

From the previous ingredient analysis, the naphtha compositions between petroleum-based and coal-based is very different, and the difference of production standard also led to the naphtha has a certain difference. So, the models put forward by the studies of existing can't be used directly. However, the previous studies can provide ideas and resources for chemical kinetic model of coal-based naphtha. H/C ratio and octane number are two very important parameters of fuel, which have important influence on lower heating value, flame propagation, combustion temperature, ignition characteristics and anti-knock property. By referring to the studies of Wang [12], Zhong [14], and Alabbad [8] etc., based on the principle of feasibility, the compositions of coal-based naphtha surrogate were selected to match the H/C ratio, RON, functional groups and average carbon chain length.

The n-alkanes and iso-alkanes are more than 95%, and cycloalkanes is only 3.784%. The n-alkanes are mainly concentrated in C_6–C_8, and iso-alkanes are mainly concentrated in C_6–C_9. Considering the average molecular formula of coal-based naphtha and existing research basis, n-heptane (NC_7H_{16}), iso-octane (IC_8H_{18}) and iso-hexane (IC_6H_{14}) can be selected. In general, considering the practicality and the cross reaction between different components, the components are selected as few as possible on the premise of accurate prediction. So, the two-components (such as PRF, n-heptane and isooctane) and three-components (such as TRF, n-heptane, isooctane and toluene) models are pretty common. Sometimes, in order to improve the

accuracy, more components (4–6 components) models have also been proposed.

This paper attempts to propose two models, the first one to match RON two-components model (n-heptane/isooctane, PRF), and the second one is a three-components model (n-heptane, isooctane, and isohexane). Because the iso-alkanes of real coal-based naphtha exceed 75%. In the calculation of RON, the methods proposed by Knop et al. [21] and Kalghatgi et al. [22] were mainly referred and obtained by weighted calculation in accordance with the proportion. Wang [12] mentioned that the calculation method of component proportion by matching H/C ratio and RON was more accurate. The first model is a simple two-components model to match the RON of coal-based naphtha, so the proportions of n-heptane and iso-octane are 46% and 54% (by mole) respectively, i.e., PRF54. The second model is a three-components model of 42.561% NC_7H_{16}, 43.683% IC_8H_{18} and 13.756% IC_6H_{14} (all by mole) with H/C ratio, RON and the sum of the three components equal to 1. Table 2 shows a comparison of coal-based naphtha with the different models constructed. It can be seen that compared with PRF54, the H/C ratio and average molecular weight of 3-components model are closer to coal-based naphtha.

Table 2. Comparison of coal-based naphtha and its surrogate.

Items	Coal-Based Naphtha	PRF54 Model	3-Components Model
RON	54	54	54
H/C ratio	2.274	2.265	2.274
Average molecular weight	102.6	107.6	104.27
n-Paraffins (mole%)	20.182	46	42.561
Iso-paraffins (mole%)	75.641	54	57.439
Olefins (mole%)	0.000	0.000	0.000
Naphthenes (mole%)	3.784	0.000	0.000
Aromatics (mole%)	0.000	0.000	0.000

2.3. Auto-Ignition Delay Time Measurements

All IDT measurements in this study were performed on an optical RCM at the University of Leeds. The Leeds RCM has been continuously improved on the basis of the original equipment to make it more suitable for engine related research. In addition, improvements in piston damping and data acquisition have improved the quality of raw data. More details can be found in the reference [23].

2.4. Coal-Naphtha HCCI Combustion on LUPOE Engine

The LUPOE (Leeds University Ported Optical Engine) research engine was employed, which typically operates under boosted conditions incorporated with a Photron SA1.1 high-speed camera and a commercially supplied Litron laser for accurate flow capture and measurement using the Particle Image Velocimetry technique. Coal-naphtha was employed for studying flame and flow characteristics in HCCI mode at a lean mixture. The coal-naphtha fuel was tested on the LUPOE research engine with an effective compression ratio 11.40. To operate on HCCI mode, the spark trigger input connection to the ignition system was disabled. In the typical operation of the research engine, the spark trigger input is integral in the timing events of the data logger, camera recording, and laser firing. However, in the current setup on HCCI mode, since the onset of combustion is determined by pressure and temperature rather than a spark trigger, the recording camera was set to be triggered by the spark signal at an advanced crank angle where the pressure and temperature were low and insufficient for autoignition to occur. The camera frame rate was set at 10 kHz, and the number of images taken is synchronized with the timing interval to determine precisely when combustion initiates. Besides the scenarios mentioned above, the research engine is similar condition as detailed in [24].

3. Analysis of Chemical Reaction Mechanism

3.1. IDTs of Single Component

From the surrogate formulation, it can be seen that the components of both PRF54 model and 3-components model are C_6-C_8. The mechanism of many small molecules has been widely studied and verified, but the mechanism of some large molecules still needs to be further studied. In this study, the Lawrence Livermore National Laboratory (LLNL) Detailed Gasoline mechanism, which is commonly used in macromolecules was applied [25]. Before using the constructed model for simulation, it is necessary to analyze and verify the single component in the model. Therefore, the ignition delay times (IDT of NC_7H_{16}, IC_8H_{18} and IC_6H_{14} were simulated and compared with the existing experiment values to verify the accuracy of the chemical reaction mechanism. The comparison results of IDT simulation and experiment values of NC_7H_{16}, IC_8H_{18} and IC_6H_{14} are shown in Figures 1–3.

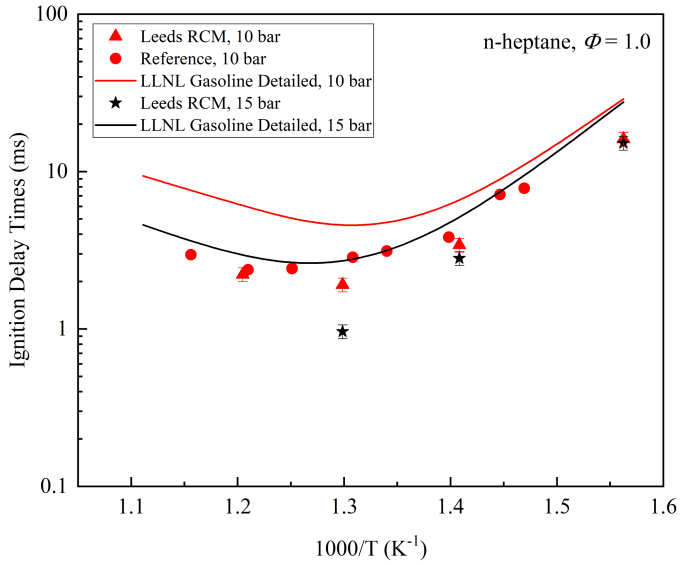

Figure 1. Experimental and simulated ignition delay times of NC_7H_{16}.

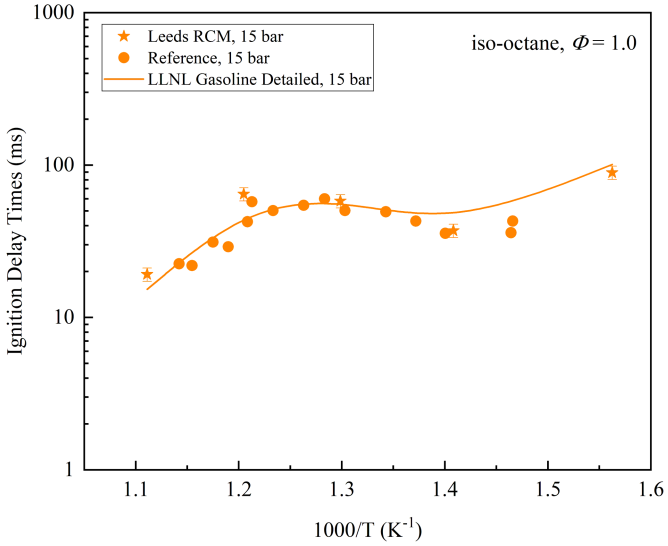

Figure 2. Experimental and simulated ignition delay times of IC_8H_{18}.

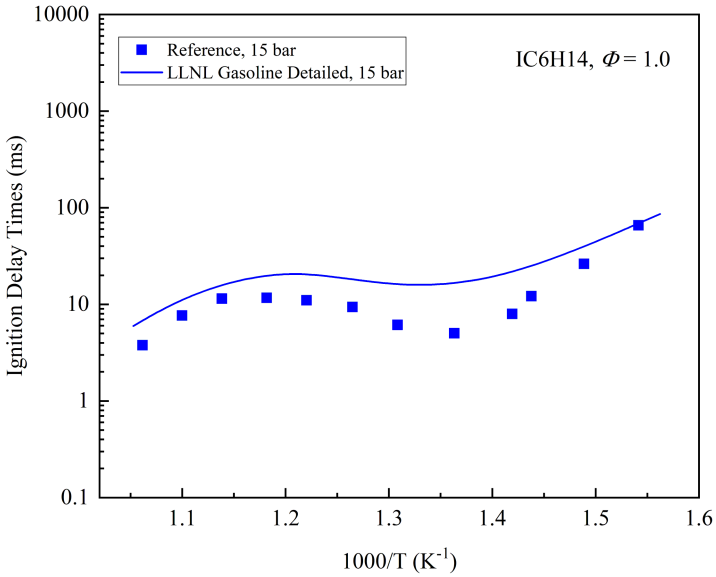

Figure 3. Experimental and simulated ignition delay times of IC_6H_{14}.

It can be seen that the LLNL Gasoline Detailed mechanism was in great discrepancy with the experiment results of reference and Leeds RCM when simulating the IDT of NC_7H_{16} at either 10 bar or 15 bar pressure. The IDT measured by Leeds RCM is significantly smaller than the simulated value. Therefore, the temperature sensitivity analysis of n-heptane was conducted to adjust the LLNL Gasoline Detailed mechanism. The simulation results of IC_8H_{18} are in good agreement with the experimental results of reference and Leeds RCM. The simulation results of IC_6H_{14} basically predicted the experiment law of the reference, but the overall IDT results were larger than the experiment values, especially in the NTC range of 690–800 K. However, considering that the simulation results of IC_6H_{14} can basically reflect the law of its experiment values, and there is a relatively obvious NTC phenomenon, the reaction mechanism related to IC6H14 is not adjusted.

3.2. Sensitivity Analysis

The temperature sensitivity analysis of NC7H16 at the pressure of 15 bar, equivalent ratio of 1.0 and temperature of 710 K, 770 K and 830 K are shown in Figures 4–6, respectively. According to the results of sensitivity analysis, the two reaction equations with great influence on the reaction rate: $NC_7H_{16} + O_2 <=> C_7H_{15-3} + HO_2$ and $C_7H_{15}O_{2-2} <=> C_7H_{14}OOH_{2-4}$ need to be adjusted. It can be seen from the previous analysis that the IDT simulated value of LLNL Gasoline Detailed mechanism in the temperature range of 710–830 K was obviously larger than the experimental value, so it is necessary to amplify the chemical reaction rate related to NC_7H_{16}. Finally, the pre-exponential factor A of the reaction equation $NC_7H_{16} + O_2 <=> C_7H_{15-3} + HO_2$ was amplified by 10 times, and the pre-exponential factor A of $C_7H_{15}O_{2-2} <=> C_7H_{14}OOH_{2-4}$ was amplified by 20 times.

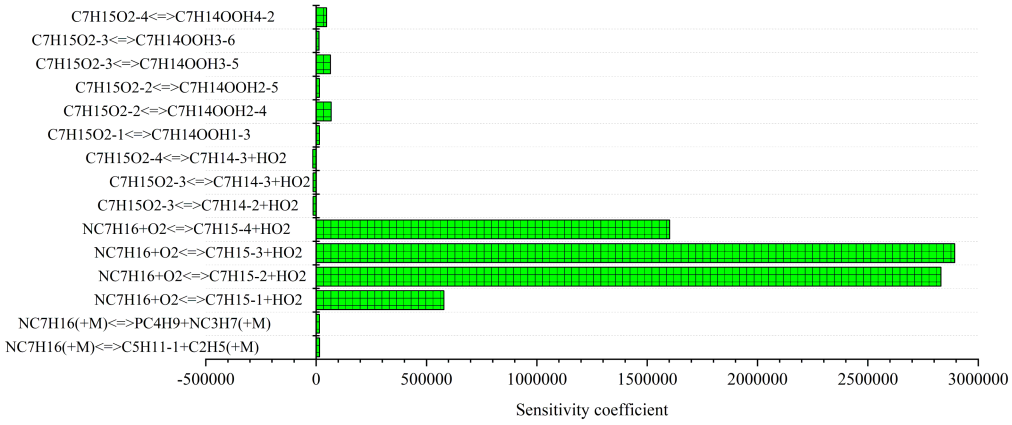

Figure 4. Sensitivity analysis of NC_7H_{16} at the pressure of 15 bar, equivalent ratio of 1.0 and temperature of 710 K.

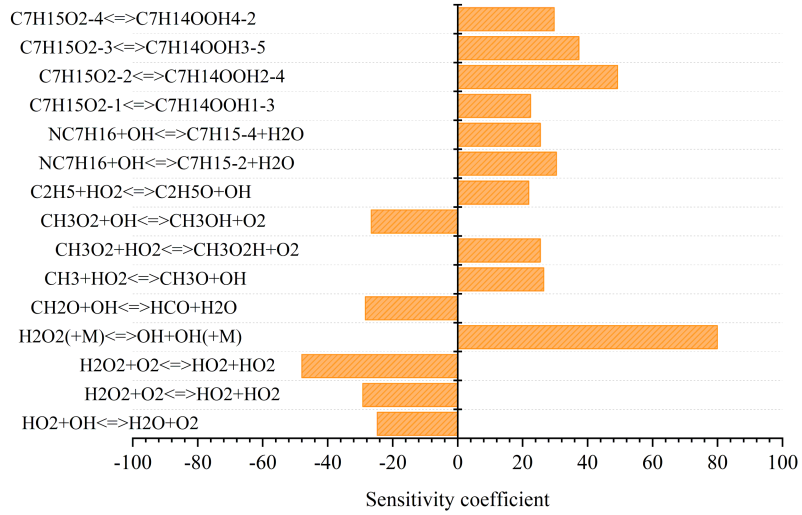

Figure 5. Sensitivity analysis of NC_7H_{16} at the pressure of 15 bar, equivalent ratio of 1.0 and temperature of 770 K.

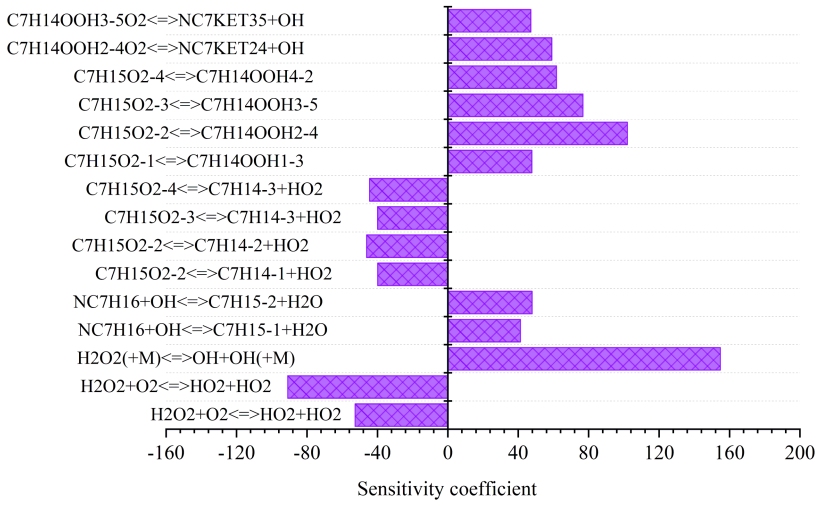

Figure 6. Sensitivity analysis of NC_7H_{16} at the pressure of 15 bar, equivalent ratio of 1.0 and temperature of 830 K.

4. Results and Discussion

4.1. Single Component Verification

The modified reaction mechanism was used to calculate the IDT of a single component, and the results were compared with the experimental data to verify the single component. The results are shown in Figure 7. It can be seen that when calculating the IDT of NC_7H_{16}, compared with the LLNL Gasoline Detailed mechanism, the calculated results of the modified mechanism are in better agreement with the experimental data. The modified mechanism can better predict the IDT law of NC_7H_{16}. When calculating the IDT of IC_8H_{18} and IC_6H_{14}, the calculated results of the LLNL Gasoline Detailed mechanism completely overlapped with the modified mechanism, and the two lines overlapped as one. This is because the equation related to NC_7H_{16} is adjusted, and IC_8H_{18} and IC_6H_{14} are not affected. Therefore, before and after adjusting the mechanism, the IDT calculated results of IC_8H_{18} and IC_6H_{14} hardly changed. This indicates that the modified mechanism can better predict the IDT of NC_7H_{16}, and does not change the calculated results of IC_8H_{18} and IC_6H_{14}. It is verified that the modified mechanism is reliable for the prediction of single component.

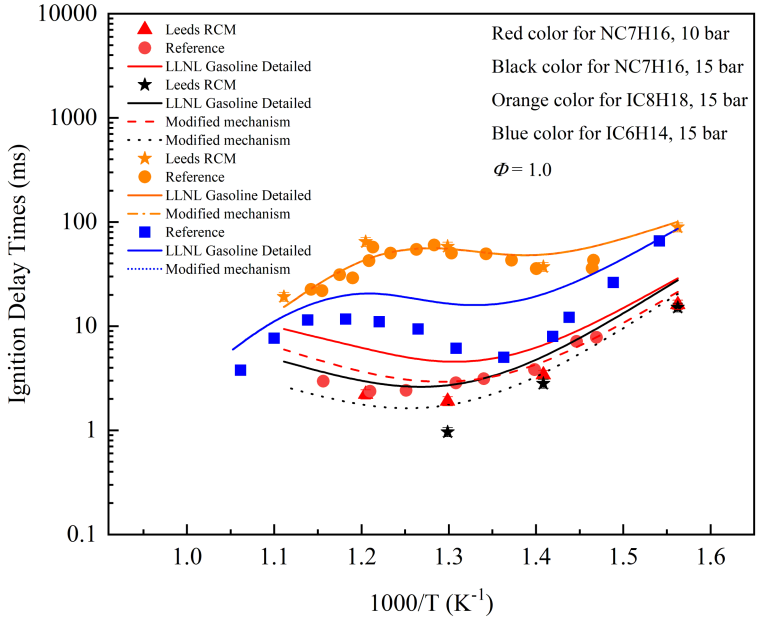

Figure 7. The single component IDT verification of modified mechanism.

4.2. Ignition Delay Times

Measured ignition delay times of coal-based naphtha (CBN) are compared with chemical kinetic simulations of PRF 54 and 3-components model. Figure 8 shows the comparison between the experimental data of CBN on a rapid compression machine (RCM) and the IDT simulation of the two models. At pressure of 10 bar and temperature of 640–900 K, the calculated results of the two models are generally consistent with the experimental results of CBN. At 15 bar, the results of the two models generally capture the law of CBN experimental results. However, the fly in the ointment is that, compared with the experimental data, both models show a slower reaction rate except at the low temperature of 640 K. This may attribute to the fact that the IDT simulation results of NC_7H_{16} are slightly larger than the experimental data. In addition, the calculated results of the two models at each temperature were generally the same, showing quite similar reactivity, whether at 10 bar or 15 bar. For low octane fuels CBN, the 3-components model shows no advantage over the 2-components model. The 2-components PRF54 model shows good prediction for the IDT of CBN when only RON is matched, which indicates that matching RON is very important in surrogate construction. Of course, the composition of the CBN is also important, since the CBN is mostly composed of alkanes (more than 95%). It should be pointed out that because the previous IDT simulation results of IC_6H_{14} are slightly larger than the experimental data, the simulation results show slower reactivity. Therefore, IC_6H_{14},

as part of the 3-components model, may have an impact on the overall reactivity, so that it does not show an advantage over PRF54 model.

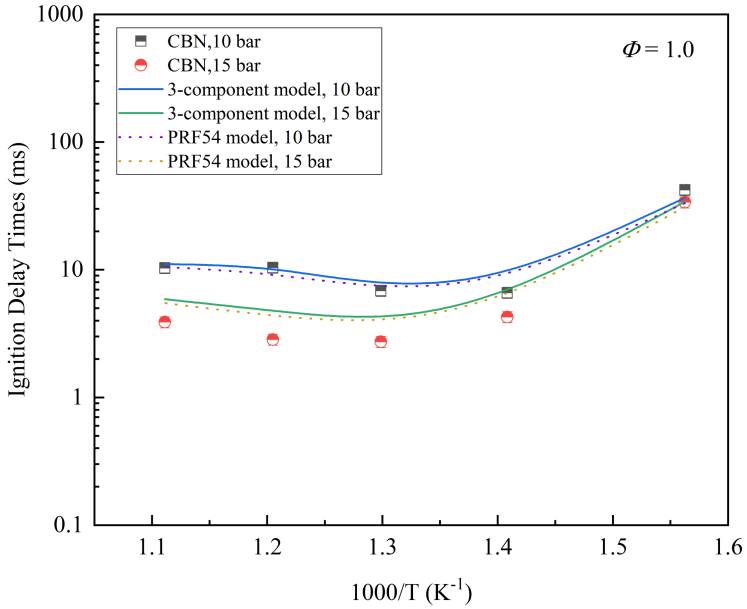

Figure 8. Comparison between measured and simulated ignition delay times.

4.3. Low-Temperatures Chemical Kinetic Analysis

A low-temperatures chemical kinetic analysis was performed to better understand the low temperature ignition behavior of CBN. Figure 9 shows the predicted hydroxyl (OH) and hydroperoxyl (HO_2) time-history curves of stoichiometric mixtures of two models (PRF 54 and 3-components model) at 15 bar and 640 K. Previous studies [8, 26 – 29] have shown that the distribution of OH radicals can help us understand the chemical kinetics of the ignition process. The initial growth patterns of OH and HO_2 radicals are similar in both models, but the growth of OH radicals in the 3-components model is slower than that of PRF54 at ~34.1 ms. The OH radical concentration of PRF54 shows a local maximum before the main ignition event, corresponding to the first-stage ignition delay time. Compared with PRF 54, the OH concentration of the 3-components model increases slowly at the beginning, but then increases rapidly, resulting in the absence of the first-stage ignition delay time. The HO_2 radicals show a similar pattern.

Temperature, OH and HO_2 sensitivity analyses of stoichiometric mixtures of 3-components model at 15 bar and 640 K are shown in Figure 10a – c. It can be seen that the overall reactivity is sensitive to the extraction of H from fuel molecules by OH radicals. NC_7H_{16} + OH appears to have the highest sensitivity coefficient and promote the overall reactivity.

In addition, the rate of production (ROP) analyses of OH and HO_2 species are performed using the 3-components model, see Figure 11a,b. The analyses indicate that the reaction of H + O_2 contributes to the production rate of OH, and CO + OH inhibits the production rate of OH. H + O_2O + OH and CO + OH <=> CO_2 + H are the two reactions that have the biggest impact on the production rate of OH. The reactions of H + O_2(+M) <=> HO_2(+M) and HO_2 + H <=> OH + OH have the biggest impact on the production rate of HO_2. The reaction of H + O_2(+M) contributes to the production rate of HO_2, and HO_2 + H inhibits the production rate of HO_2.

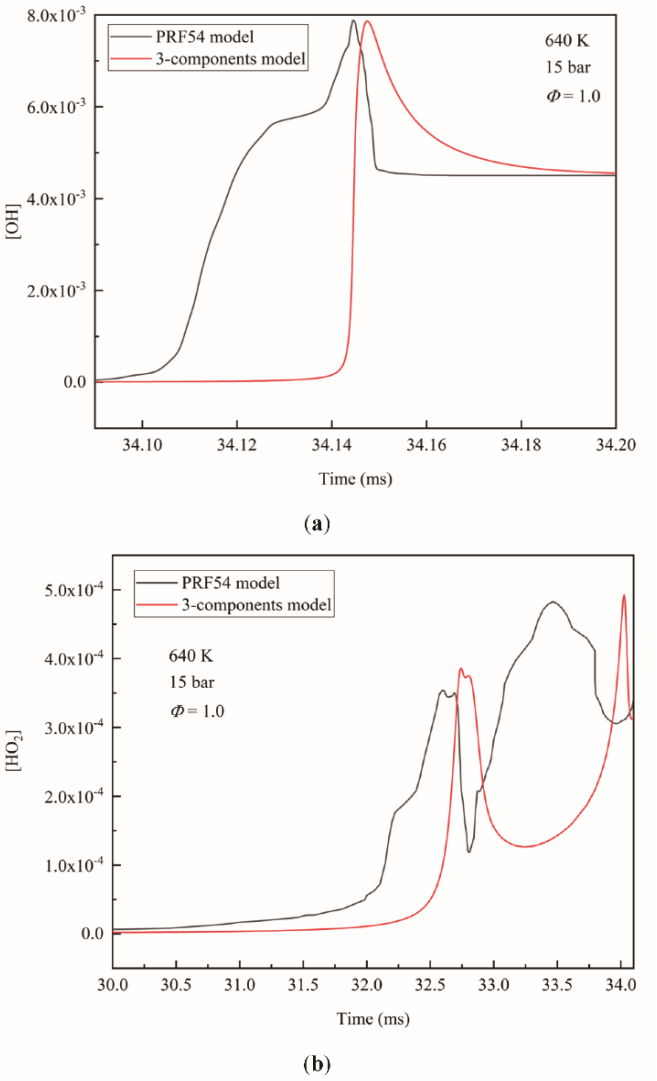

Figure 9. OH (**a**) and HO_2 (**b**) concentration-time history during the oxidation of PRF54 and 3-components model.

Compared with PRF54, the content of NC_7H_{16} in the 3-components model is similar to that in PRF54, but the IC_6H_{14} is added. Interestingly, the overall reactivity of IC_6H_{14} is better than that of IC_8H_{18}, but the 3-components model does not show a significant advantage. There are probably two main reasons for this: First, it can be seen from the previous sensitivity analysis results that the reaction between NC_7H_{16} and OH has the highest sensitivity coefficient and promotes the overall reactivity in the low-temperature reaction stage. So, the NC_7H_{16} is the most important fuel component that affects the reaction rate. However, at higher temperatures, the fuel composition has little effect because the oxidation process is mainly the decomposition of H_2O_2 to form two OH radicals and the chain branching reaction of $H + O_2$ [8]. Secondly, the simulated IDT results of the IC_6H_{14} are longer than the real experimental results, especially in the NTC region.

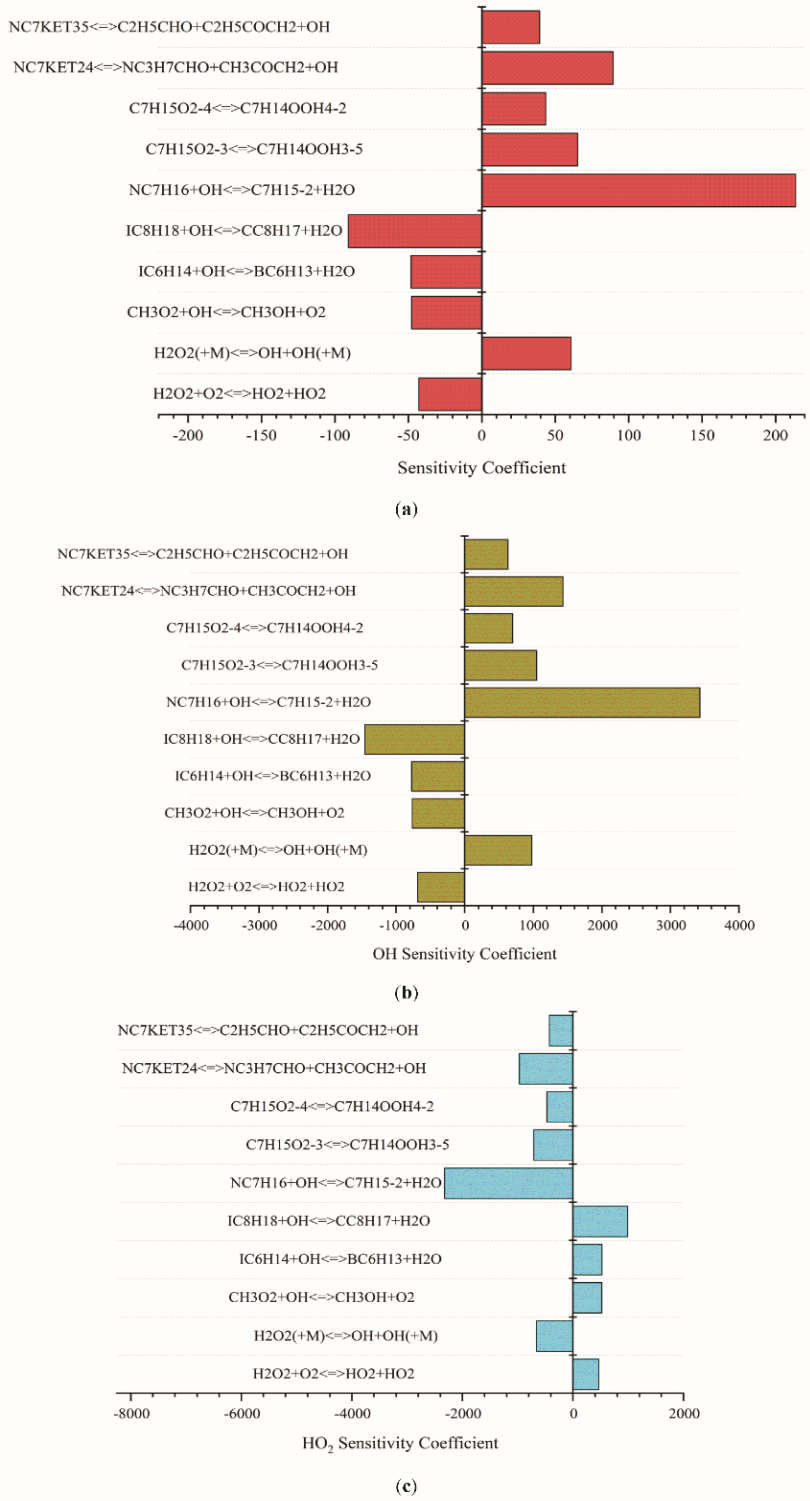

Figure 10. Sensitivity analysis for (**a**) temperature, (**b**) OH, (**c**) HO_2.

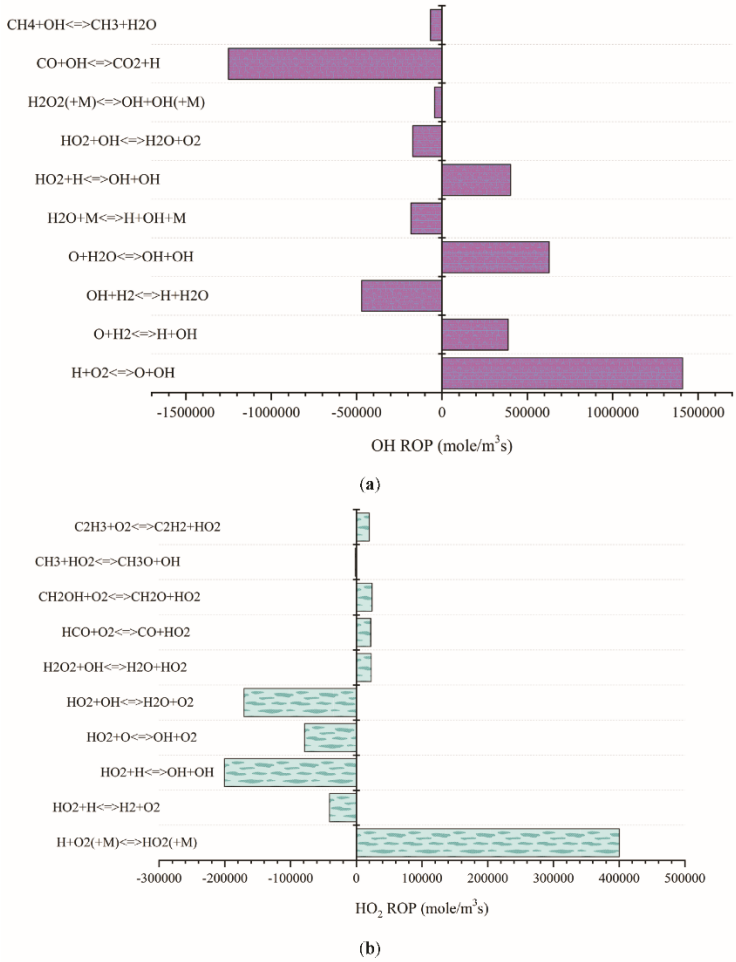

Figure 11. Rate of production analysis, (**a**) OH, (**b**) HO_2.

4.4. Coal-Naphtha HCCI Engine Simulations

4.4.1. Model Validation

Based on the mechanism of PRF54 and 3-components model, ic_engine_hcci_adiabatic module of Chemkin-Pro was used to simulate the coal-based naphtha HCCI engine. The effects of T_{in} and Φ on combustion of 3-components model HCCI were studied. The engine compression ratio is 18.3:1 and engine speed is maintained at a constant 1200 r/min. More details about original engine parameters are provided in Table 3.

Table 3. Original engine parameters.

Items	Parameters
Type	4JK1
Cylinder diameter × stroke	95.4 × 87.4 mm
Compression ratio	18.3
Type of cooling	Water-cooling
Displacement	2.499 L
Maximum torque	320 N·m
maximum output power	100 kW

As can be seen from Figure 12, compared with the experimental results, the in-cylinder pressure simulated by the zero-dimensional single-zone model of the coal-based naphtha HCCI established in this study is in good agreement with the experimental results in terms of the shape of the overall pressure curve and the prediction of the combustion starting point, especially in the low-temperature oxidation process, except for certain deviations in the peak pressure and combustion phase. This is because the HCCI model does not consider the heat transfer process and heat loss, so the calculated value of the peak pressure is larger than the experimental value. However, the relative error is within the allowable range, and the trend of pressure change is completely consistent, so the model can be considered reliable and effective. In addition, before the spontaneous combustion of the mixture, the calculated in-cylinder pressure is very close to the experimental value, but the calculated pressure in the high-temperature combustion stage near the top dead center is slightly larger than the experimental data, mainly because the single-zone model is used in the calculation process, and the influence of the temperature stratification in the cylinder and the concentration stratification of the mixture on the combustion process is not considered, resulting in the calculated result being too large. However, the single-zone model can represent the area with the highest temperature in the entire combustion chamber, so it can accurately predict the ignition timing of the fuel, and this study mainly focuses on the prediction of the ignition of the coal-based naphtha. In the prediction of HCCI model, the combustion phase of the experimental value will be slightly earlier than that of the calculated value. Based on the comparison between the simulated and the experimental value, the IDT of coal-based naphtha in the experiment is smaller than the simulated value, which is corresponding to the results of HCCI. In addition, since the test is using a naturally aspirated engine, the actual intake pressure should be less than 1 atm due to the pump air loss. In terms of ignition delay and cumulative heat release, the experimental ignition of naphtha is slightly earlier than the simulated, as the combustion progresses, under the comprehensive influence of heat loss, boundary conditions and ideal single-zone model, the cumulative heat release simulated is greater than the experimental value. This is not only reflected during peak in-cylinder pressure, but also shows a significant trend as in-cylinder pressure begins to decrease. This is a good explanation for the combustion phase problem. It is worth mentioning that the HCCI simulation results of PRF54 and 3-components model are almost identical.

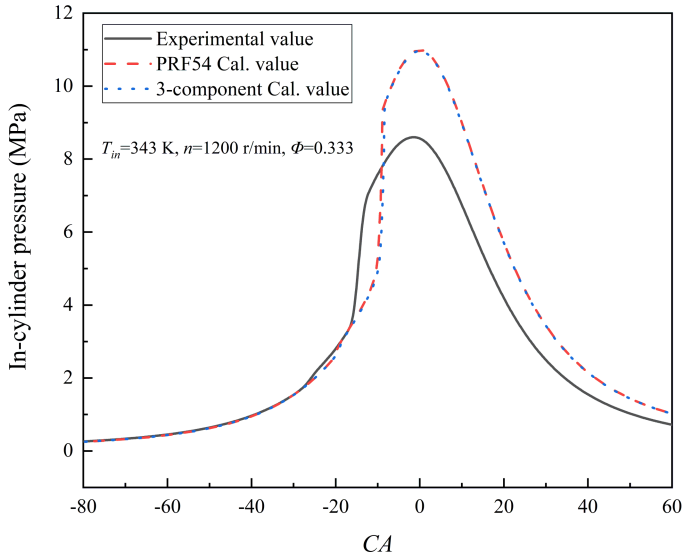

Figure 12. Comparison of the calculated in-cylinder pressure with the experimental data.

4.4.2. Effect of T_{in}

The intake temperature is one of the key boundary conditions affecting the combustion characteristics of HCCI. This section mainly studies the effect of intake temperature on the OH and HO_2 radical concentrations in the cylinder under engine speed n = 1200 r/min and Φ = 0.333. The results are calculated using 3-components model.

Figures 13 and 14 show the effect of T_{in} on the variation of in-cylinder OH and HO_2 radical concentrations, respectively. As can be seen from the figure, both OH and HO_2 mole fraction gradually increase with the increase of temperature. The increase of the initial temperature increases the number of activated molecules and the probability of intermolecular collision, thus speeding up the reaction rate of each elementary element in the low temperature reaction stage of the coal-based naphtha, and promoting the formation of these two radicals. It can be seen that with the increase of T_{in}, the mole fraction of the two radicals increases advance with the change of crank angle. The reason is that when T_{in} increases, the temperature in the cylinder increases, which increases the active free radicals and is conducive to the formation of OH radical. Subsequently, the increase of OH concentration promotes the formation of HO_2 radicals.

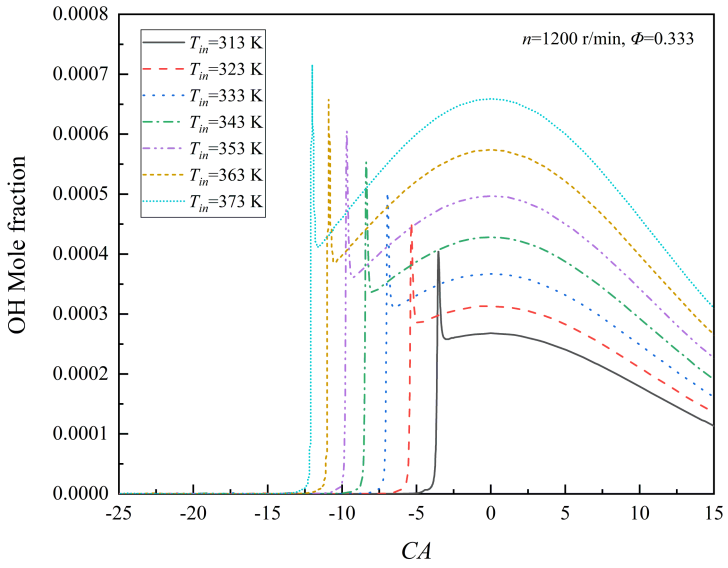

Figure 13. Effect of T_{in} on OH mole fraction.

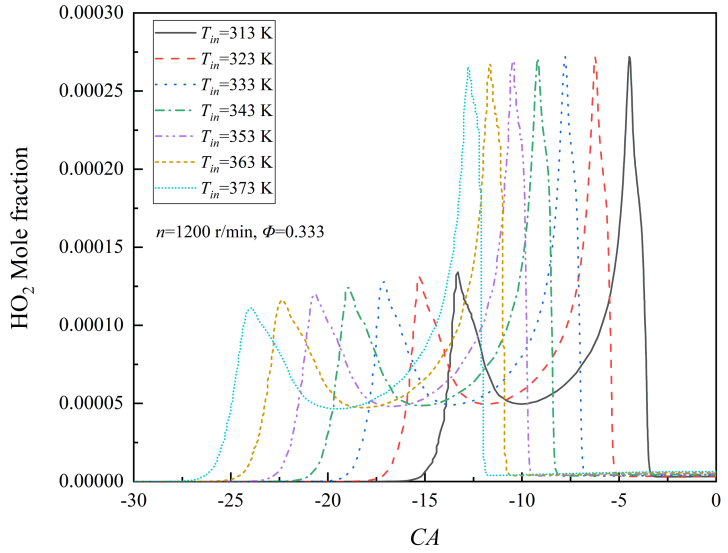

Figure 14. Effect of T_{in} on HO_2 mole fraction.

4.4.3. Effect of Φ

Load expansion has always been the difficulty of HCCI engine technology, and the parameter directly related to it is the equivalent ratio. In this section, the effect of the change of in-cylinder mixture

concentration on OH and HO_2 mole fraction is studied by changing the equivalent ratio in the initial parameters of the 3-components model under n = 1200 r/min and T_{in} = 313 K.

Figures 15 and 16 show the effect of Φ on the variation of in-cylinder OH and HO_2 concentrations, respectively. It can be seen from the figure that in the low temperature reaction stage, the mole fractions of OH and HO_2 change little when the Φ changes. Although the generation rate of the two radicals increases under the influence of the increase of the reactant concentration, the related consumption reaction rate also increases, and the change of the concentration also changes the reaction path of the related primitive. Finally, the concentration of the two radicals changes little with the increase of Φ in the low temperature reaction stage. In addition, the effect of Φ on combustion phase is small. The combustion of coal-based naphtha HCCI is more sensitive to the T_{in}.

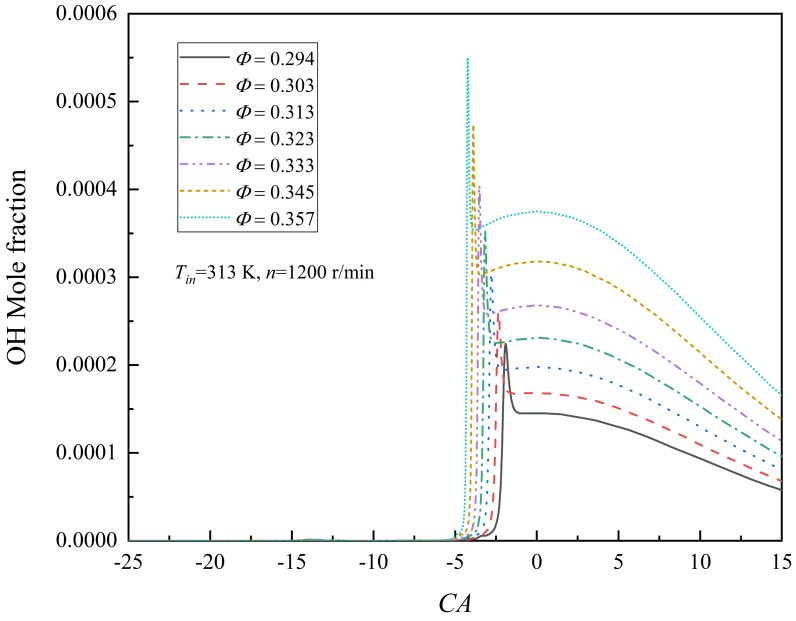

Figure 15. Effect of Φ on OH mole fraction.

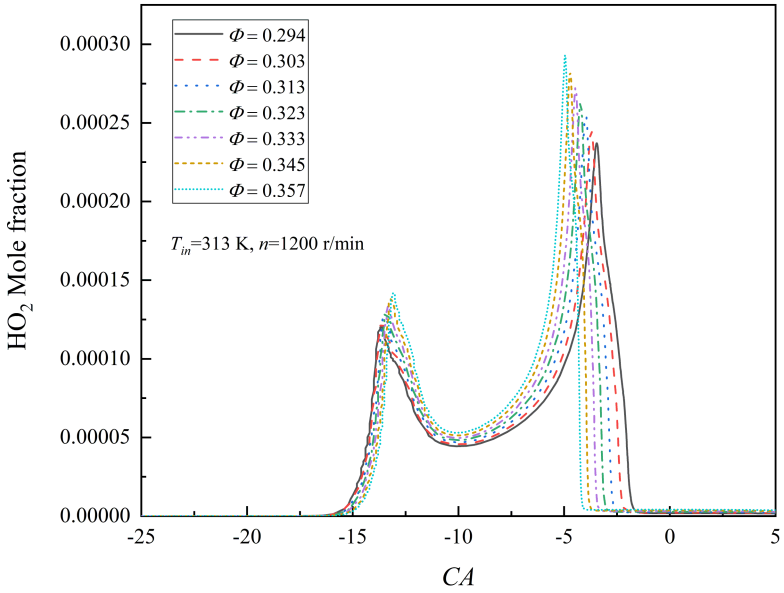

Figure 16. Effect of Φ on HO_2 mole fraction.

4.5. Coal-Naphtha HCCI Combustion Images

In order to enrich the research on coal-based naphtha HCCI combustion and gain a deeper understanding of the combustion process in the cylinder, based on the Leeds optical engine, the optical images of HCCI fueled with naphtha has been performed. With the successful achievement of HCCI in the research engine, an optical head was installed for image diagnostics. Three cycles of imaging were acquired under lean conditions, with an engine speed of 750 rpm, intake airflow rate of 5.18 g/s, and a camera frame rate of 10 kHz, resulting in a time between frames of 0.1 s.

From the flame luminous images captured and a cycle displayed in Figure 17, it was observed that ignition occurs simultaneously in multiple locations involving gradual conversion of fuel. However, it was observed that large bright intensities first appear near the cylinder wall, indicating initial autoignition in these regions before more autoignition events occur closer towards to center. This observation is in contrast to spark-ignited PIV data, where a central spark ignites a homogeneous mixture, leading to a flame kernel initiated from the center of the domain and propagating outward radially. The engine intake manifold and cylinder barrel are heated to 323.15 K to vaporize the fuel and increase temperature in the combustion chamber to encourage autoignition respectively. This led to a temperature gradient where the walls are at a higher temperature compared to center of the engine cylinder. In HCCI mode, where the fuel-air mixture is uniformly compressed, these hot surfaces near the walls can lower the local ignition delay, leading to earlier autoignition in these regions.

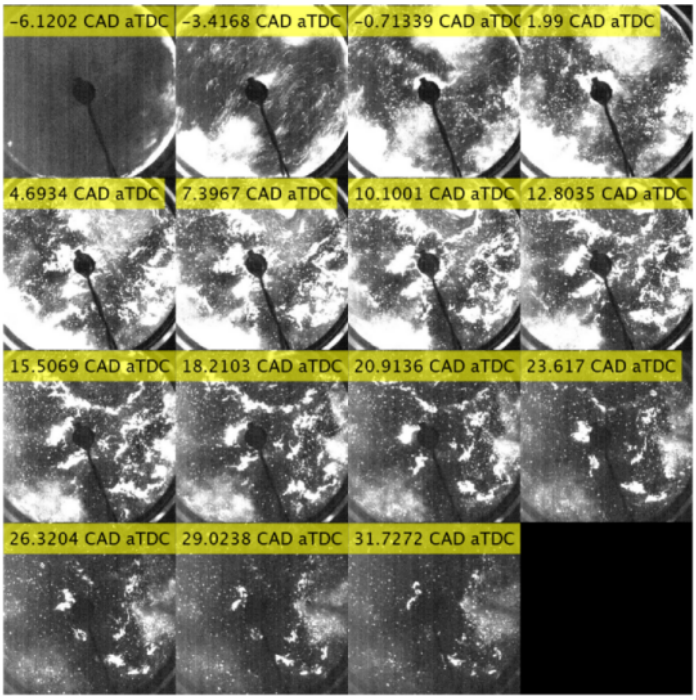

Figure 17. LUPOE HCCI, fueled by CBN at 750 rpm, Φ = 0.7, Effective compression ratio = 11.40. Skipped every 3 instances for clarity.

5. Conclusions

In this paper, the chemical kinetics model of a coal-based naphtha (RON54) was studied. Considering the complex compositions of a coal-based naphtha, its fuel properties and detailed hydrocarbon compositions were analyzed. And according to the analysis results, two surrogate models (PRF54 and 3-composition model) were built to simulate the IDT of real coal-based naphtha. Firstly, the experimental data (IDTs) of single component was used to verify the LLNL mechanism. Then, IDT for a coal-based naphtha was measured in Leeds RCM. The simulation results of two surrogate models were compared with experimental data. The results show that at pressure of 10 bar and temperature of 640–900 K, the IDT simulation results of the two models are generally consistent with the experimental results of CBN. And at 15 bar pressure, the

IDT simulation results of the two models generally capture the law of CBN experimental results. However, the fly in the ointment is that, compared with the experimental data, both models show a slower reaction rate except at the low temperature of 640 K. The IDT simulation results show slower reactivity, and the 3-component model shows no advantage over the PRF54 model. Sensitivity analyses indicate that the overall reactivity is sensitive to the extraction of H from fuel molecules by OH radicals. NC_7H_{16} + OH appears to have the highest sensitivity coefficient and promote the overall reactivity. The ROP analyses indicate that the reaction of H + O_2 contributes to the production rate of OH, and the reaction of H + O_2(+M) contributes to the production rate of HO_2.

In addition, the experimental and simulation study of coal-based naphtha HCCI combustion was carried out. CHEMKIN-PRO software was used to simulate the effects of intake temperature (T_{in}) and equivalent ratio (Φ) on the combustion process of naphtha HCCI engine. The results show that the combustion of coal-based naphtha HCCI is sensitive to the T_{in}. With the increase of T_{in}, the combustion phase of HCCI is obviously advanced, the concentration of OH and HO_2 increases in the middle and low temperature reaction process, and the corresponding curve moves forward as a whole. The change of Φ has little effect on the concentration of OH and HO_2 before ignition, and the change of ignition time with the mixture concentration is not obvious. It should be pointed out that when the T_{in} is high or mixture is rich, the coal-based naphtha HCCI engine is prone to knock, and the peak phase will appear before top dead center (TDC). This phenomenon is especially obvious when the T_{in} is very high. It can be seen that the coal-based naphtha is suitable for low-temperature lean combustion.

Author Contributions: A. L.: methodology, software, data curation, validation, writing—original draft preparation; J.J.A.: visualization, investigation; J.Y.: conceptualization, supervision, writing—reviewing and editing. All authors have read and agreed to the published version of the manuscript.

Funding: This research received no external funding

Institutional Review Board Statement: Not applicable.

Informed Consent Statement: Not applicable.

Data Availability: Statement: Not applicable.

Conflicts of Interest: The authors declare no conflict of interest.

References

1. Javed, T.; Nasir, E.F.; Ahmed, A.; Badra, J.; Djebbi, K.; Beshir, M.; Ji, W.; Sarathy, M.; Farooq, A. Ignition delay measurements of light naphtha: A fully blended low octane fuel. *Proc. Combust. Inst.* **2017**, *36*, 315–322.
2. Chang, J.; Kalghatgi, G.; Amer ,A.; Viollet, Y. *Enabling High Efficiency Direct Injection Engine with Naphtha Fuel through Partially Premixed Charge Compression Ignition Combustion*; SAE International: Warrendale, PA, USA, 2012; *SAE* 2012-01-0677.
3. Chang, J.; Viollet ,Y.; Amer, A.; Kalghatgi, G. *Fuel Economy Potential of Partially Premixed Compression Ignition (PPCI) Combustion with Naphtha Fuel*; SAE International: Warrendale, PA, USA, 2013; SAE 2013-01-2701.
4. Yang, Y.; Dec, J.; Dronniou, N.; Sjöberg, M.; Cannella, W. Partial fuel stratification to control HCCI heat release rates: Fuel composition and other factors affecting pre-ignition reactions of two-stage ignition fuels. *SAE Int. J. Engines* **2011**, *4*, 1903–1920.
5. Han, D.; Ickes, A.M.; Assanis, D.N.; Huang, Z.; Bohac, S.V. Attainment and load extension of high-efficiency premixed low-temperature combustion with dieseline in a compression ignition engine. *Energy Fuels* **2010**, *24*, 3517–3525.
6. Han D.; Ickes, A.M.; Bohac, S.V.; Huang, Z.; Assanis, D.N. HC and CO emissions of premixed low-temperature combustion fueled by blends of diesel and gasoline. *Fuel* **2012**, *99*, 13–19.
7. Han, D.; Ickes, A.M.; Bohac, S.V.; Huang, Z.; Assanis, D.N. Premixed low-temperature combustion of blends of diesel and gasoline in a high speed compression ignition engine. *Proc. Combust. Inst.* **2011**, *33*, 3039–3046.
8. Alabbad, M.; Issayev, G.; Badra, J.; Voice, A.K.; Giri, B.R.; Djebbi, K.; Sarathy, S.M.; Farooq, A. Autoignition of straight-run naphtha: A promising fuel for advanced compression ignition engines. *Combust. Flame* **2018**, *189*, 337–346.
9. AlAbbad, M.; Badra, J.; Djebbi, K.; Farooq, A. Ignition delay measurements of a low-octane gasoline blend, designed for gasoline compression ignition (GCI) engines. *Proc. Combust. Inst.* **2019**, *37*, 171–178.
10. Javed, T.; Ahmed, A.; Lovisotto, L.; Issayev, G.; Badra, J.; Sarathy, S.M.; Farooq, A. Ignition studies of two low-octane gasolines. *Combust. Flame* **2017**, *185*, 152–159.
11. Li, J.; Zhu, J.; Wang, S.; Feng, Y.; Zhou, W.; Qian, Y.; Yu, L.; Lu, X. An experimental and modeling study of autoignition characteristics of two real low-octane gasoline fuels in a heated rapid compression machine at elevated pressures. *Fuel* **2021**, *295*, 120645.

12. Wang, B. Autoignition of light naphtha and its surrogates in a rapid compression machine. *Energy Sci. Eng.* **2019**, *7*, 207–216.
13. Ahmed, A.; Khurshid, M.; Naser, N.; Badra, J.; Gaillard, P.; Chung, S.H.; Roberts, W.L.; Sarathy, M. Surrogate fuel formulation for light naphtha combustion in advanced combustion engines. In Proceedings of the 7th European Combustion Meeting, Budapest, Hungary, 30 March–*2* April 2015.
14. Zhong, A.; Li, X.; Turányi, T.; Huang, Z.; Han, D. Pyrolysis and oxidation of a light naphtha fuel and its surrogate blend. *Combust. Flame* **2022**, *240*, 111979.
15. Lu, A.; Zhang, C.; Ren, Y.; Li, Y.; Li, S.; Yin, P. Research on knock recognition of coal-based naphtha homogeneous charge compression ignition engine based on combined feature extraction and classification. *Fuel* **2021**, *300*, 120997.
16. Xie, Y.; Lu, A.; Li, J.; Yang, J.; Zhang, C.; Morsy, M.E. Laminar burning characteristics of coal-based naphtha. *Combust. Flame* **2023**, *249*, 112625.
17. Mehl, M.; Chen, J.Y.; Pitz, W.J.; Sarathy, S.M.; Westbrook, C.K. An approach for formulating surrogates for gasoline with application toward a reduced surrogate mechanism for CFD engine modeling. *Energy Fuels* **2011**, *25*, 5215–5223.
18. Ahmed, A.; Goteng, G.; Shankar, V.S.; Al-Qurashi, K.; Roberts, W.L.; Sarathy, S.M. A computational methodology for formulating gasoline surrogate fuels with accurate physical and chemical kinetic properties. *Fuel* **2015**, *143*, 290–300.
19. Pera, C.; Knop, V. Methodology to define gasoline surrogates dedicated to auto-ignition in engines. *Fuel* **2012**, *96*, 56–69.
20. Pitz, W.J.; Cernansky, N.P.; Dryer, F.L.; Egolfopoulos, F.N.; Farrell, J.T.; Friend, D.G.; Pitsch, H. *Development of an Experimental Database and Chemical Kinetic Models for Surrogate Gasoline Fuels*; SAE International: Warrendale, PA, USA, 2007; SAE Technical Papers 2007-01-0175.
21. Knop, V.; Loos, M.; Pera, C.; Jeuland, N. A linear-by-mole blending rule for octane numbers of n-heptane/iso-octane/toluene mixtures. *Fuel* **2014**, *115*, 666–673.
22. Kalghatgi, G.; Babiker, H.; Badra, J. A simple method to predict knock using toluene, n-heptane and iso-octane blends (TPRF) as gasoline surrogates. *SAE Int. J. Engines* **2015**, *8*, 505–519.
23. Mehl, M.; Pitz, W.J.; Westbrook, C.K.; Curran H.J. Kinetic modeling of gasoline surrogate components and mixtures under engine conditions. *Proc. Combust. Inst.* **2011**, *33*, 193–200.
24. Michelbach, C.A. Ignition and heat release behaviour of iso-butanol and gasoline blended fuels: An experimental and kinetic modelling study. Ph.D. Thesis, University of Leeds, Leeds, UK, 2020.
25. Zhang, W.; Morsy, M.E.; Ling, Z.; Yang, J. Characterization of flame front wrinkling in a highly pressure-charged spark ignition engine. *Exp. Therm. Fluid Sci.* **2022**, *132*, 110534.
26. Sarathy, S.M.; Kukkadapu, G.; Mehl, M.; Javed, T.; Ahmed, A.; Naser, N.; Tekawade, A.; Kosiba, G.; AlAbbad, M.; Singh, E.; et al. Compositional effects on the ignition of FACE gasolines. *Combust. Flame* **2016,** *169*, 171–193.
27. Merchant, S.S.; Goldsmith, C.F.; Vandeputte, A.G.; Burke, M.P.; Klippenstein, S.J.; Green, W.H. Understanding low-temperature first-stage ignition delay: Propane. *Combust. Flame* **2015**, *162*, 3658–3673.
28. Singh, E.; Badra, J.; Mehl, M.; Sarathy S.M. Chemical kinetic insights into the octane number and octane sensitivity of gasoline surrogate mixtures. *Energy Fuels* **2017**, *31*, 1945–1960.
29. Lapuerta, M.; Hernández, J.J.; Sarathy, S.M. Effects of methyl substitution on the auto-ignition of C16 alkanes. *Combust. Flame* **2016**, *164*, 259–269.